PAPER

Liposomal nanoprobes that combine anti–EGFR antibodies and MRI contrast agents: synthesis and *in vitro* characterization

Yuan-Chia Kuo,[ab] Chiwei Hung,[b] Rao P. Gullapalli,[d] Su Xu,[d] Jiachen Zhuo,[d] Srinivasa R. Raghavan*[ac] and Warren D. D'Souza*[ab]

Targeted delivery of antibodies has emerged as an option for treating cancer. One antibody that is used clinically is the epidermal growth factor receptor (EGFR)-inhibiting monoclonal antibody, *Cetuximab*. EGFR is overexpressed on many tumor cell membranes, and the binding of antibodies to these receptors inhibits the proliferation and metastasis of the cancer. However, no diagnostic tools currently exist to monitor the *in situ* binding of antibodies to tumor cells in real time. To address this deficiency, we have created a liposomal probe bearing anti-EGFR antibodies and chelated gadolinium (Gd), a positive (image-brightening) contrast agent for magnetic resonance imaging (MRI). Our strategy to synthesize these probes has been carefully designed to be simple and scaleable: it employs two steps that each involve self-assembly. In the first step, biocompatible phospholipids, a chelated-Gd lipid, and a biotinylated lipid are used to form liposomes. In the ensuing step, biotinylated antibodies are attached to the liposomes using avidin as linker. The resulting probes preferentially bind *in vitro* to EGFR-overexpressing tumor cells compared to controls. Moreover, cancer cells with bound probes can be easily tracked using MRI. In the future, these probes could find clinical use for tracking the efficacy of cancer treatment in real-time by MRI.

Introduction

The cells of many cancer tumors are known to over-express receptors for growth factors, such as the epidermal growth factor receptor (EGFR), on their cell membranes.[1–5] An abundance of EGFR activates signaling pathways that ultimately leads to increased tumor proliferation, migration, and angiogenesis;[6] in turn, these cells also carry higher risk of metastasis.[7–10] Targeted therapy for some cancers taking advantage of the molecular signature of over-expressed EGFR has emerged as a therapeutic option in recent years. Simple incubation of anti-EGFR monoclonal antibodies with carcinoma cell lines has been shown to inhibit tumor growth and invasion, presumably by blocking intracellular EGFR signaling pathways.[11,12] This finding has been translated to the clinic: specifically, the FDA-approved EGFR-targeting monoclonal antibody *Cetuximab*

(Bristol-Myers Squibb, Eli Lilly & Co.) is now used directly as a therapeutic agent against head-and-neck and colorectal cancers.[10,13] Clinical trials have shown that *Cetuximab* in combination with radiotherapy improved the 5 year overall survival rate of squamous cell carcinoma head and neck (SCCHN) patients to 46%, compared with 36% for the radiotherapy-only group.[10] When combined with chemotherapy, *Cetuximab* lengthened the median overall survival time from 7.4 to 10.1 months.[14]

While the protocols for treating cancers with *Cetuximab* are well-established, clinicians currently cannot directly assess the *in vivo* effectiveness of such targeted agents over the course of a multi-week treatment regimen. Computed tomography (CT), positron emission tomography (PET), and magnetic resonance imaging (MRI) are the most useful live imaging technologies for cancer evaluation.[15] Among these methods, MRI is advantageous in that it provides high-resolution details and better contrast for discriminating between normal and tumor tissue, especially when used in conjunction with contrast agents. Contrast agents for MRI fall into two categories: negative-contrast (image-darkening) agents like iron oxide and positive-contrast (image-brightening) agents, such as gadolinium (Gd). The negative-contrast agents have limitations in detecting tumors since the airways surrounding tumors may yield dark signals as well, making it difficult to differentiate tumor from air in images. In comparison, positive-contrast

[a]*Fischell Department of Bioengineering, University of Maryland, College Park, MD 20742, USA*

[b]*Department of Radiation Oncology, University of Maryland School of Medicine, 22 South Greene St., Baltimore, MD 21201, USA. E-mail: wdsou001@umaryland.edu; Tel: +1 (410) 328-7074*

[c]*Department of Chemical and Biomolecular Engineering, University of Maryland, 1227C, Chem-Nuc Building 090, College Park, MD 20742, USA, +1 (301) 405-8164. E-mail: sraghava@umd.edu*

[d]*Department of Diagnostic Radiology & Nuclear Medicine, University of Maryland School of Medicine, Baltimore, MD 21201, USA*

agents like Gd are preferred. Gd^{3+} is a strong paramagnetic ion that shortens the T_1 and T_2 relaxation times of nearby water protons, thereby providing an increased signal on the MR image.[16–19] While free Gd^{3+} ions are quite toxic,[20,21] their toxicity can be sufficiently lowered by complexing Gd^{3+} ions with chelating compounds such as diethylenetriamine–pentaacetic acid (DTPA).[22–27] The standard clinical injection dose of Gd–chelates is about 0.1–0.3 mmol kg^{-1}, which results in an average concentration of 0.5 mM in the extracellular space.[24,28]

To observe EGFR-overexpressing cancer cells *via* MRI following targeted therapy, we have focused on constructing a nanoscale probe bearing both anti-EGFR antibodies and a positive MRI contrast agent, *i.e.*, chelated Gd. Such a probe would be able to home in on tumor cells due to the antibodies, while the Gd would allow the corresponding area to be seen clearly on the MR image. For such a probe to be useful *in vivo*, it would have to be nontoxic and of overall size ~100 to 200 nm, which is optimal for *in vivo* circulation and concentration within tumors. Moreover, we wanted to develop a probe-synthesis method with as few steps as possible and using commercially available ingredients. The rationale was that a simple method would be scalable and allow synthesis of the probe in sufficient quantities to be eventually used in the clinic. These constraints led us to select liposomes as the optimal choice of nanoscale vehicle. Liposomes formed from phospholipids are much less toxic compared to other alternatives such as cationic dendrimers.[29] Moreover, they can be formed in a single step *via* self-assembly, which is a much simpler process than that required typically for polymer-based nanoparticles.

We report in this paper the engineering of liposomes that are non-covalently conjugated with both Gd–DTPA as well as *Cetuximab*, the therapeutic anti-EGFR antibody. The synthesis strategy is presented in Fig. 1 and discussed further below. The resulting mutlifunctional liposomes are studied *in vitro* and shown to exhibit preferential binding to EGFR-rich SCCHN cells compared to low-EGFR-expressing cells. Moreover, we demonstrate the ability to track these structures using MRI. Overall, these liposomes are a promising class of structures for tracking EGFR-overexpressing cancer cells in real time by MRI.

Experimental section

Chemicals

1,2-Dipalmitoyl-*sn-glycero*-3-phosphocholine (DPPC); 1,2-dioleoyl-*sn-glycero*-3-phospho-ethanolamine-*N*-(biotinyl) (sodium salt) (DOPE–Biotin); DTPA-bis(stearylamide) (gadolinium salt) (Gd–DTPA–bSA); and 1,2-dioleoyl-*sn-glycero*-3-phosphoethanolamine-*N*-[methoxy(polyethyleneglycol)-2000] (DOPE-mPEG) were purchased from Avanti Polar Lipids Inc. 1,1′-Dioctadecyl-3,3,3′,3′-tetramethyl-indocarbocyanine perchlorate (DiI) was purchased from Molecular Probes. Cholesterol, chloroform, and methanol was obtained from Sigma-Aldrich (St. Louis, MO). Premixed WST-1 cell proliferation reagent was purchased from Clontech. Sulfosuccinimidyl-6-[biotinamido]-6-hexanamidohexanoate (Sulfo-NHS-LC-LC-Biotin) and the corresponding biotin quantification kit were obtained from Thermo Fisher Scientific Inc.

Gd-liposome preparation

For Gd-liposome preparation, a lipid mixture consisting of DPPC, cholesterol, Gd–DTPA–bSA, DOPE–mPEG, and DOPE–biotin (molar ratio 30 : 39.9 : 25 : 5 : 0.1) was dissolved in a chloroform–methanol (4 : 1 v/v) mixture.[30] Fluorescent liposomes were created by including 2 μM DiI. A dried film was formed by evaporating the solvent with a dry nitrogen stream, followed by vacuum desiccation for 24 h. The dried lipid film was rehydrated with water in 8 mM concentration and stirred at 60 °C for 2 h. The mixture was then ultrasonicated at 47.5 W for 15 min using a probe sonicator (Qsonica, Newtown, CT) to give unilamellar liposomes. pH was adjusted to 7.4 using PBS and samples were maintained at 4 °C before the experiments.

CAGE probe synthesis

8 mL of 2 mg mL^{-1} *Cetuximab* (anti-EGFR antibody from Bristol-Myers Squibb) was purified using Sephadex G-25 column chromatography (GE Healthcare). Purified protein was analyzed by measuring OD at 280 nm using a NanoDrop 1000 (Thermo Fisher Scientific Inc.). To conjugate cetuxmiab with biotin, the sulfo-NHS–LC–LC–Biotin was mixed with the purified *Cetuximab* and agitated at 4 °C for 24 h and purified *via* Sephadex G-25 column chromatography. The biotin quantification kit was used for measuring the biotin per *Cetuximab*. Finally, the biotinylated *Cetuximab* was combined with Gd-liposomes (at a 1 : 4 ratio of biotins on the antibody compared to the liposomes), and the tetrameric protein, avidin (from Sigma-Aldrich) was added at a molar ratio of 1 : 50 for avidin–total biotin.

Size measurement

Vesicle size was measured by Dynamic Light Scattering (DLS) (Photocor Instruments). A 5 mW laser light source at 633 nm was used to analyze the size of vesicles. Studies were done at 25 °C with the scattering angle being 90°. All measurements were conducted in triplicate.

Zeta potential

Surface potentials of vesicles were measured by a Laser Doppler Velocimetry technique (Malvern Zetasizer Nano ZS90) at a 90° scattering angle. Samples were placed in disposable polystyrene cuvettes (Folded Capillary Cell-DTS1060, Malvern). All measurements were conducted in triplicate.

Transmission Electron Microscopy (TEM)

Samples were characterized by TEM on a Jeol JEM 2100 microscope at a 80 kV accelerating voltage. Carbon/formvar coated copper grids (Ted Pella, Inc.) were dipped into the solution containing the vesicle samples and then placed in a fume hood for 5 min. The dried TEM grids were then stained with a drop of 1% uranyl acetate (from Sigma-Aldrich) solution and the resulting grids were air-dried before taking images.
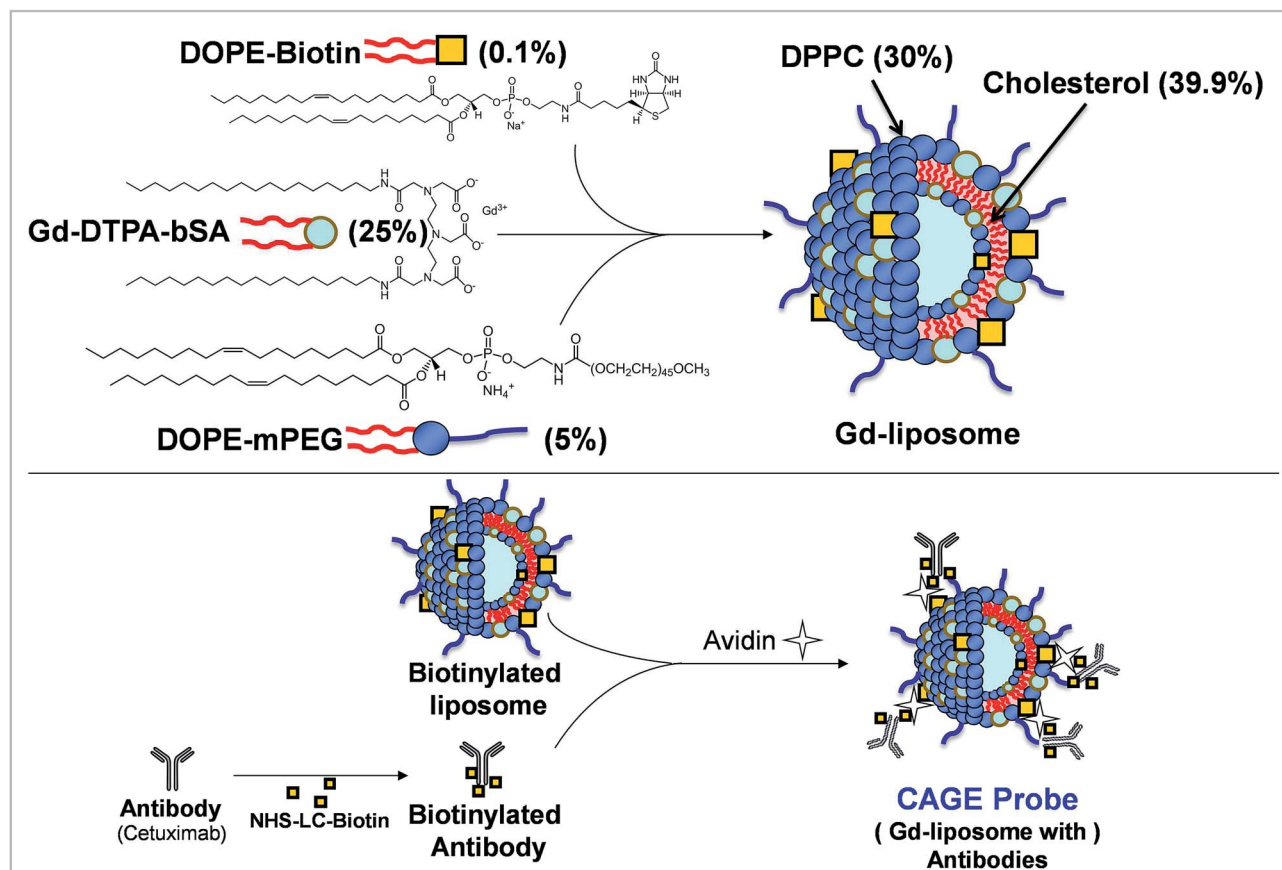
Fig. 1 Structure of CAGE probes with chelated Gd and antibodies to EGFR within a single structure of size ~100 nm. (Top) The lipids DPPC, cholesterol, Gd–DTPA–bSA, DOPE–mPEG, and DOPE–biotin are combined to produce Gd-liposomes. (Bottom) The Gd-liposomes are combined with biotinylated *Cetuximab* (anti-EGFR antibody) and the tetrafunctional protein, avidin. The antibodies get attached to the Gd-liposomes *via* biotin–avidin interactions to form the CAGE probe. "CAGE" includes chelated Gd and antibodies to EGFR.

MR properties of the liposome

For T_1-weighted MR imaging, the samples (Gd-liposome/CAGE probe) were transferred to a 2 mL Eppendorff tube. Inversion recovery pulse sequence was used for the measurement of T_1 relaxation time by the least-squares algorithm using a 3.0 Tesla Siemens MAGNETOM-Trio system at 25 °C with the following settings: echo time (TE) = 12 ms, repetition time (TR) = 6000 ms. Thirteen different inversion-recovery waiting delay values (TI) between 40 ms and 2800 ms were measured (slice thickness = 5 mm). The signal intensity of each tube in the MRI was measured by placing a region of interest in the center of the cross-sectional images of the tube under different TI. T_1 values of each tube were calculated by fitting the collected data to the following function: $f(x) = m(1 - 2 \exp(-TI/T_1))$ using Matlab, where $f(x)$ is the corresponding signal intensity and the fitting parameters are m and T_1. A plot of $1/T_1$ *versus* Gd^{3+} concentration yielded a straight line with the slope being the samples' T_1 relaxivity value r_1.

Cell lines

SCCHN 15B cells were provided by Dr Jennifer Grandis (University of Pittsburgh) and HEK293 human embryonic kidney cells were purchased from American Type Culture Collection. Cells were cultured in DMEM medium for HEK293 (Invitrogen) or RPMI-1640 medium for 15B with 10% FBS (Hyclone), 1% L-glutamine (Sigma-Aldrich) and maintained at 37 °C and 5% CO$_2$. Cells were propagated to 80% confluency prior to the *in vitro* assay. Phosphate buffered saline (PBS) was purchased from Invitrogen.

Flow-cytometry analysis of EGFR expression

HEK and 15B were incubated at 37 °C for 1 h with Alexa Fluor labeled anti-EGFR antibody, sc-120 AF488 (green fluorescence, purchased from Santa Cruz Biotechnology, CA) at dilutions of 1/1000 and 1/3000 with PBS. Excess antibody was removed from the cells by washing three times with PBS and 5×10^5 cells were collected in 500 μl PBS. EGFR expression for each cell line were analyzed by counting cells emitting green fluorescence by a FACScan (Becton-Dickinson). Additionally, Alexa Fluor signals in the cells were directly visualized by fluorescence microscope (Olympus BX60).

Cell viability

Cells were plated in 96-well plates at a density of 10^4 cells per well containing 100 μL of culture medium; after 24 h of cultivation, the cells were incubated with varying concentrations of

vesicles. After 24 h of incubation, cell viability was evaluated by MTT assay using Premix WST-1 cell proliferation reagent (Clontech), and measuring the absorbance at 440 nm by a SpectraMax M2 spectrometer (Molecular Devices). All experiments were performed in triplicate.

Cell targeting and competition assays

10^4 cells were seeded onto an 8 well chamber slide. After overnight culture, cells were blocked with a culture medium containing 1% BSA at 37 °C for 30 min, and the CAGE probe or Gd-liposome was added at 2 mg mL^{-1} for 2 h of incubation at 37 °C. After washing with PBS three times, the samples were fixed with 2% paraformaldehyde, and slides were mounted with antifade, 4′,6′-diamidino-2-phenylindole (DAPI)-containing fluorescent mounting media (EMD Chemicals), and visualized under a fluorescence microscope. For the competition assay, 15B cells were incubated with 1 : 50 sc-120 AF488 antiEGFR antibody at 37 °C for 40 min, washed with PBS, and then incubated with different concentrations of CAGE probe for 1 h in a 37 °C incubator. After the same fixation steps above, slides were prepared and stored at 4 °C. The fluorescence intensity evaluation was done by ImageJ software (NIH). After manually selecting the region containing cells, total fluorescence intensity was acquired. To get the average fluorescence intensity per cell, the total intensity was divided by the number of cells. The result is the specific fluorescence intensity, which represents the average intensity of each cell.

Liposome targeting assay by MRI

15B cells were cultured in several T175 flasks. In one flask, 12 mL of CAGE probe in cell medium (corresponding to 6 mM Gd^{3+}) was added. In another flask, 12 mL of Gd-liposomes in cell medium (also corresponding to 6 mM Gd^{3+}) along with free Cetuximab (equal to that in the flask with the CAGE probe) was added. Each flask was incubated for 1 h at 37 °C. The same process was repeated with additional cell-bearing flasks. Thereafter, all the cells were collected by centrifugation and washed three times with PBS. The cells were then fixed with 4% paraformaldehyde for 20 min at 4 °C. Then, the cells were placed in Eppendorff tubes for MR screening. The MR protocol is the same as described above to evaluate the Gd concentration bound to cells.

Results and discussion

Preparation of multifunctional liposomal nanoprobes

The base liposomal formulation employed here is a mixture of the phospholipid DPPC and cholesterol. We sought to conjugate both Gd–DTPA and antibodies to such liposomes. Towards this end, three additional lipids were introduced into the formulation, as shown in Fig. 1. The first lipid, Gd–DTPA–bSA, has Gd–DTPA bound to two stearyl tails by amide linkages. The second lipid, DOPE–biotin, has two oleyl tails and a biotin attached to the lipid headgroup. A third lipid, DOPE–PEG was also added to the formulation; this lipid has two oleyl tails and a polyethylene glycol (PEG) oligomer (2000 Da) attached to the

headgroup. The five molecules, *i.e.*, DPPC, cholesterol, Gd–DTPA–bSA, DOPE–PEG, and DOPE–biotin were combined at a molar ratio of 30 : 39.9 : 25 : 5 : 0.1 for a typical formulation, with the overall lipid concentration being 6 mg mL^{-1} or 8 mM. Liposomes were prepared by sonication and we refer to the overall structures as Gd-liposomes. Note that the DOPE–PEG provides PEG chains on the exterior of the liposome, which impart steric stability and are expected to enhance the *in vivo* circulation time.[31]

The size and stability of Gd-liposomes were evaluated using dynamic light scattering (DLS). Liposome diameters for the typical composition noted above were measured to be 100 nm, 120 nm, respectively (Fig. 2) and the sizes remained unchanged over three weeks of observation. The proportion of the Gd–DTPA–bSA lipid had an impact on liposomal stability. Since a higher fraction of Gd–DTPA–bSA in the liposomal bilayer would yield an increased signal in MRI, we attempted to increase this fraction (while reducing the cholesterol fraction). However, if the Gd–DTPA–bSA fraction was raised above 25 mol%, the liposomal diameter increased substantially over time (data not shown), and in some cases, precipitation was observed. These observations indicate aggregation or destabilization of the liposomes. For these reasons, we fixed the Gd–DTPA–bSA fraction at 25 mol%.

The above Gd-liposomes had a zeta potential of +5.13 mV in water, indicating a net cationic nature. Among the lipids used, DPPC is zwitterionic and cholesterol is nonionic. The PE headgroups in DOPE–PEG and DOPE–biotin are anionic, but the fractions of these lipids in the formulation is low (5 and 0.1 mol%, respectively). Thus, the cationic nature of the overall liposomes is evidently arising from the Gd–DTPA–bSA lipid, and more specifically from the Gd^{3+}. The weak positive charge on the liposomes may be beneficial as it can provide electrostatic repulsions between them, which helps to stabilize the liposomes. The Gd-liposomes were also studied in PBS buffer and were again found to be stable over time. However, measurements of the zeta potential in buffer did not yield consistent values, possibly because of the screening of electrostatic interactions by the ions in PBS. Thus, stability in PBS may be
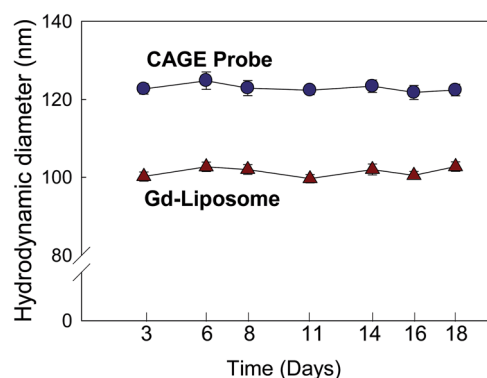
Fig. 2 Liposome size and stability over a period of 18 days. Data are shown for Gd-liposomes (no antibody) and for the CAGE probes (liposomes with antibody attached). The sizes correspond to the hydrodynamic diameters from DLS.

attributed primarily to steric repulsions from the PEG side chains. TEM images of Gd-liposomes – negatively stained by uranyl acetate (Fig. 3a and b) show that these liposomes are unilamellar spheres with diameters around 100 nm, which is broadly consistent with the DLS data above.

We then proceeded to attach antibodies to the Gd-liposomes. The antibody chosen was *Cetuximab*, the therapeutic anti-EGFR antibody, and we first chemically affixed biotins to it by the reaction shown in Fig. 1. Each *Cetuximab* acquired ∼3 biotins by this reaction. The biotinylated *Cetuximab* was then combined with the Gd-liposomes (bearing DOPE–biotin) in the presence of avidin, a tetrameric biotin-binding protein. A molar ratio of overall biotin:avidin = 50 : 1 was used and the ratio of biotins on Gd-liposomes *versus* biotins on *Cetuximab* was kept at 1 : 4. The components were mixed by agitation for 40 min and then maintained at 4 °C. In the process, *Cetuximab* becomes bound to the liposomes, as shown in Fig. 1. We use the term "CAGE" to refer to the final liposomal structures since they combine chelated Gd as well as antibodies to EGFR. The CAGE probes were characterized by DLS (Fig. 2) and TEM (Fig. 3c and d). Fig. 2 shows that the CAGE probes were also around 100 nm in diameter. They were slightly larger than the Gd-liposomes. This finding is consistent with antibody conjugation. TEM also reveals that the CAGE probes are unilamellar liposomes with sizes consistent with those measured by DLS.

Quantification of MR contrast

Next, we quantified the MR signal of the above structures using a 3 T scanner. These studies were done with the Gd-liposomes and the CAGE probe. Gd–DTPA solutions were used as the standard for comparison. The longitudinal relaxation times T_1 for Gd-liposomes, the CAGE probe and Gd–DTPA solutions were measured at various dilutions. Plots of $1/T_1$ *versus* $[Gd^{3+}]$ for all sets of samples follow straight lines (Fig. 4). The inverse relationship confirms that the higher the $[Gd^{3+}]$, the shorter the relaxation time T_1. The slopes of the lines are defined as the relaxivities r_1 for each class of samples. r_1 was 3.3 mM^{-1} s^{-1} for Gd–DTPA solutions, 8.07 mM^{-1} s^{-1} for the Gd-liposomes and 3.93 mM^{-1} s^{-1} for the CAGE probe. The r_1 values of Gd-liposomes and CAGE probes were 2.4 and 1.19 times higher
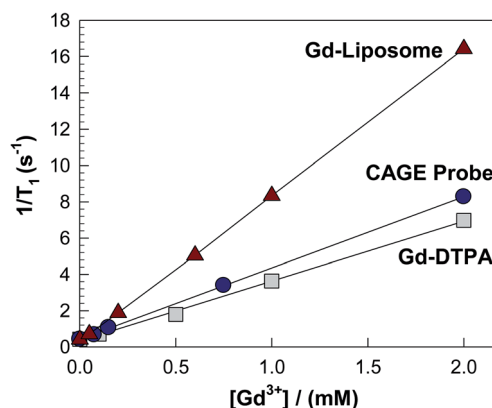

Fig. 4 Relaxivity plots of $1/T_1$ *vs.* Gd^{3+} from MR measurements. Plots are shown for solutions of Gd–DTPA as well as for solutions containing Gd-liposomes. The slopes of the lines give the relaxivities for each sample (Gd-liposomes: r_1 = 8.07 mM^{-1} s^{-1}, CAGE probe: r_1 = 3.93 mM^{-1} s^{-1} and Gd–DTPA: r_1 = 3.3 mM^{-1} s^{-1}).

than that of Gd–DTPA, respectively. This implies that the Gd-bearing nanostructures give rise to greater MR contrast than Gd–DTPA. The r_1 enhancement for the Gd-liposomes may be the result of their being embedded in bilayers,[32] which restricts the internal (rotational) motion of Gd. Higher relaxivity due to restricted internal motion of Gd has been reported previously.[33,34] The CAGE probe may have decreased r_1 compared with Gd-liposomes because the linkage of avidin and the biotinylated antibody may shield the Gd in the liposomal bilayer from interactions with water, which would decrease the density of Gd-coordinated water molecules. It is worth noting that the T_1 time for water is 2383 ms and it is 2252 ms for the bare liposomes without Gd (negligible difference). In comparison, the inclusion of the Gd–DTPA–bSA lipid in the liposomes at a concentration of 2.0 mM reduces the T_1 time to 61 ms. This difference between bare and Gd-liposomes (2252 ms to 61 ms) is large enough to give appreciable contrast in MR images.

EGFR expression: SCCHN *vs. normal* cells

As noted in the Introduction, most SCCHN cell lines are known to over-express EGFR, and one such cell line is the 15B line.[35,36] We used SCCHN 15B as the positive control in targeting assays with our CAGE probes. For comparison, a human embryonic kidney cell line (HEK 293) was used to represent normal cells with low EGFR expression. To confirm that SCCHN 15B cells exhibited higher EGFR expression levels compared to HEK 293 cells, each type of cells was contacted with an anti-EGFR antibody (sc-120 AF488) conjugated with the green fluorescent moiety, Alexa Fluor. Thereafter Alexa Fluor-positive cells were analyzed by flow cytometry and fluorescence microscopy. As expected,[37,38] HEK 293 cells exhibited very low levels of EGFR expression with only 2.8% Alexa Fluor-positive cells detected by flow cytometry and almost no Alexa Fluor signal (green) in the fluorescence micrograph (Fig. 5a). On the other hand, SCCHN 15B cells exhibited high expression levels of EGFR with nearly 100% of cells detected as Alexa Fluor-positive in flow cytometry
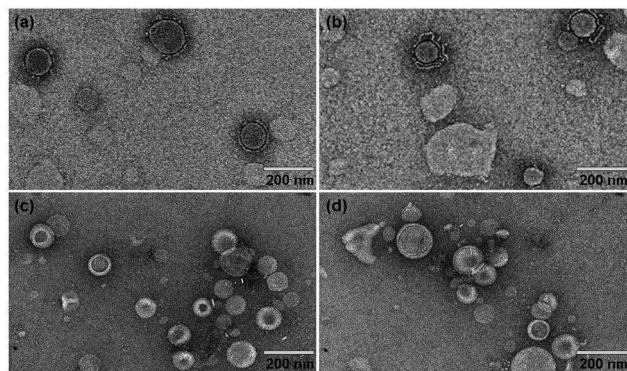

Fig. 3 TEM images of liposome structures stained with 1% uranyl acetate. (a and b) Gd-liposomes; (c and d) CAGE probes.

(Fig. 5b). These results confirmed the distinctive expression levels of EGFR between 15B and HEK 293 cells.

Cytotoxicity of CAGE probe on SCCHN 15B cells

Before proceeding to the targeting assay, the cytotoxicity of the Gd-liposomes and the CAGE probes was investigated. SCCHN 15B cells were incubated with different concentrations of Gd-liposomes or CAGE probes for 24 h and the fraction of surviving viable cells was determined by the MTT assay. The data are presented in Fig. 6. In the case of Gd-liposomes, more than 80% of cells remained viable at liposome concentrations between 0.01 to 1 mg mL^{-1}, while 50% of cells survived at 5 mg mL^{-1}. The assay thereby validates that the Gd-liposomes as relatively nontoxic, and this finding has also been confirmed by other researchers for similar liposomes.[39,40] Compared with Gd-liposomes, the CAGE probes showed some toxicity to cells: 70% of cells remained viable at a probe concentration of 1 mg mL^{-1} while 20% of cells survived at a concentration of 3 mg mL^{-1}.

Targeting ability of CAGE probes

To evaluate the targeting ability of CAGE probes, we chose a concentration of 2 mg mL^{-1}. The procedure for the experiment was based on that used by Mulder et al.[41] and was designed to test whether the CAGE probes could specifically target EGFR-over-expressing cells. Gd-liposomes (no conjugated antibody) were used as the control. To assess targeting by fluorescence microscopy, an additional fluorescent lipid probe (DiI) was added to the liposomal bilayers of both the CAGE and the Gd-
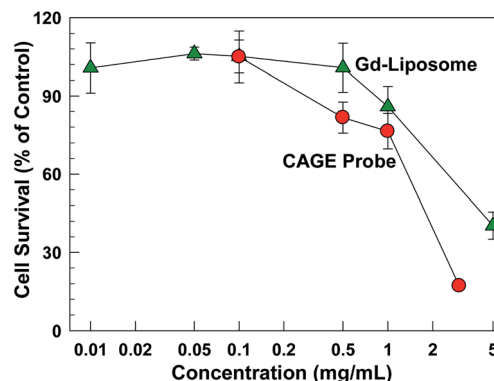

Fig. 6 Cell viability (MTT) assay of 15B cells incubated with different structures. Gd-liposomes show low toxicity to cells, while the CAGE probes are somewhat toxic above 2 mg mL^{-1}.

liposomes. We used live HEK 293 and SCCHN 15B cells for the targeting experiments. The experiments involved incubating the cells with the probes (or the controls) for 2 h, followed by washing to remove unbound probes, and then imaging of the cells for fluorescence from DiI. Although the probes were somewhat toxic at this concentration over the 24 h time period in the MTT assay (Fig. 6), they are not expected to significantly affect the cells over the shorter incubation time of 2 h in the targeting experiments.

The results of the targeting experiments are shown by the fluorescence micrographs in Fig. 7. The red color in the images indicates fluorescence from DiI in the liposomal membranes. As expected, the Gd-liposomes gave a similar weak red signal for both the SCCHN and normal cell lines, indicating that these liposomes randomly bind to cells without specificity (Fig. 7a and b). On the other hand, in the case of the CAGE probes, a significantly higher signal was observed with the EGFR-over-
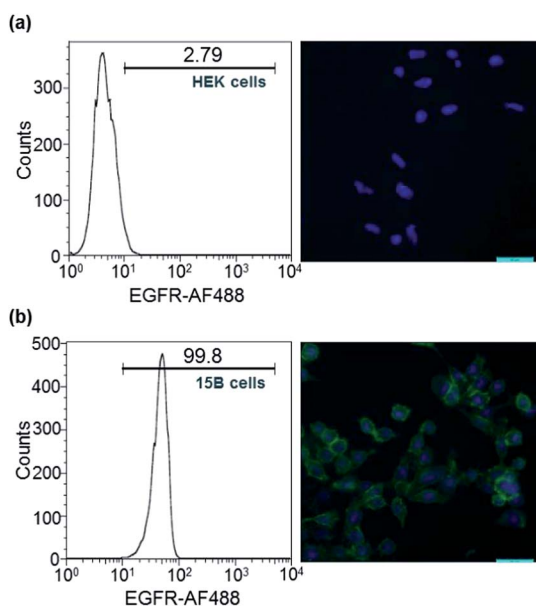

Fig. 5 EGFR expression of normal HEK cells compared with that of SCCHN 15B cells by flow cytometry and fluorescence microscopy. (a) Very low Alexa Fluor fluorescence signal (green) is observed with HEK cells (2.79%) which implies low levels of EGFR expression. (b) In comparison, a high Alexa Fluor signal is found for 15B cells (99.8%). Note that in the micrographs, the cell nucleus stained by DAPI gives blue fluorescence, while the Alexa Fluor-bound antibody gives green fluorescence.
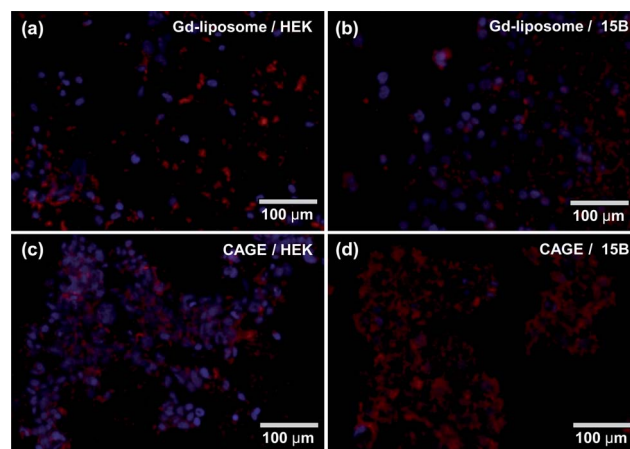

Fig. 7 EGFR-mediated binding of Gd-liposomes and CAGE probes by HEK and 15B cells. Since the Gd-liposomes do not have any targeting function, they show some non-specific binding to both HEK cells (a) and 15B cells (b). On the other hand, the CAGE probes are able to bind significantly more to EGFR-overexpressing 15B cells (d) compared to HEK cells (c).

expressing SCCHN 15B cells compared to the normal HEK 293 cells (Fig. 7c and d). These results indicate cell specificity and membrane binding of the CAGE probe against the 15B cells. The differences in fluorescence signals were quantified using ImageJ software. For the CAGE probes combined with 15B cells, the specific fluorescence intensity (per cell) was 41 ± 7. In comparison, for the CAGE probes with HEK 293 cells, the intensity (per cell) was 12 ± 6. Lastly, for the Gd-liposomes together with 15B cells, the intensity (per cell) was 14 ± 6. Thus, there is a 3-fold higher fluorescence per cell in the case of the CAGE probe incubated with 15B cells, relative to the two controls. This higher signal is evidently a result of binding of the CAGE probe to EGFR receptors on the 15B cells.

Competitive targeting of CAGE *vs.* anti-EGFR antibody

To further evaluate the targeting ability of CAGE probes, we conducted a competition assay using the CAGEs against the anti-EGFR antibody (sc-120 AF488) (used also for EGFR quantification by flow cytometry). First, SCCHN 15B cells were incubated with the sc-120 antibody, which resulted in a strong green signal due to Alexa Fluor (green fluorescence) around the cells (Fig. 8a). The same cells were contacted with a low concentration (0.1 mg mL^{-1}) of CAGE for 1 h, whereupon, the Alexa Fluor signal decreased and a dim red signal due to DiI in the CAGE was barely visible (Fig. 8b). When the CAGE probes were added at medium concentration (0.8 mg mL^{-1}), the Alexa Fluor signal decreased further and a clear red signal from the CAGE became visible (Fig. 8c). Finally, when a high concentration of CAGE (2 mg mL^{-1}) was introduced, the Alexa Fluor signal was nearly eliminated and all cells showed a distinctive red envelope, showing the binding of CAGE probes (Fig. 8d). These results clearly show that the affinity of CAGE probes for EGFR on 15B cell membranes is comparable to that of the sc-120 antibody.

Sample	Water	0.5 mM Gd-DTPA	15B bound Gd-Lipo	15B bound with CAGE
T_1 (ms)	2383	381.4	516.2	379.3

Fig. 9 MRI screening of CAGE probe-targeted 15B cells. T_1 values and MR images at TI = 1000 ms for pure water, 0.5 mM Gd–DTPA, Gd-liposome and CAGE probe-targeted 15B cells. T_1 values were calculated based on the intensity inside the circle by adapting a curve fitting tool in Matlab.

In vitro study of CAGE-targeted 15B cells using MRI

Finally, we used MRI to screen a sample of 15B cells with bound CAGE probes. For this experiment, 15B cells were combined with CAGE probes at a concentration of 5 mg mL^{-1} (0.5 mM Gd) and incubated for 1 h. The cells were then washed with buffer to remove unbound CAGE, fixed and placed in an Eppendorf tube for MRI scanning. For comparison, we also scanned tubes containing water and a 0.5 mM solution of Gd–DTPA. The corresponding cross-sectional images are shown in Fig. 9; these images correspond to an inversion time, TI = 1000 ms. From images corresponding to various inversion times, the T_1 relaxation times were calculated. The water sample has a T_1 of 2252 ms, consistent with the relatively dark image. The 0.5 mM Gd–DTPA solution, in comparison, has a much lower T_1 of 381.4 ms, which reflects the much brighter image. The conjugate of Gd-liposome (which serves as a control with 0.5 mM Gd) incubated with 15B cells, resulted in a T_1 of 516.2 ms, which is 1.5 times higher than the Gd–DTPA solution. Finally, the 15B cells with bound CAGE probe yielded a T_1 of 379.3 ms, which is similar to the T_1 of 0.5 mM Gd–DTPA. The level of contrast in this image is more than sufficient for imaging purposes. Thus, we conclude that our Gd-bearing CAGE probes are capable of providing MRI images with sufficient resolution if the probes can effectively bind to their targets. Future studies will examine these probes *in vivo* using animal models of SCCHN.

Conclusions

In this study, we have developed CAGE probes as a class of biocompatible nanostructures capable of binding selectively to cells that have an over-abundance of EGFRs on their membranes. Simultaneously, the CAGE probes are decorated with Gd–DTPA–bearing lipids, which enables them to provide positive contrast in MR images to regions with high levels of probe binding. In preparing these probes, we have deliberately chosen a simple, two-step procedure that uses materials that are commercially available, biologically-derived, biocompatible and non-toxic. The procedure involves self-assembly of a mixture of five lipids: DPPC, cholesterol, a lipid with Gd–DTPA, a PEGylated lipid, and a biotinylated lipid to yield liposomes of ~100 nm diameter. Thereafter, in a second self-assembly step, the above liposomes are combined with biotinylated *cetuximab*
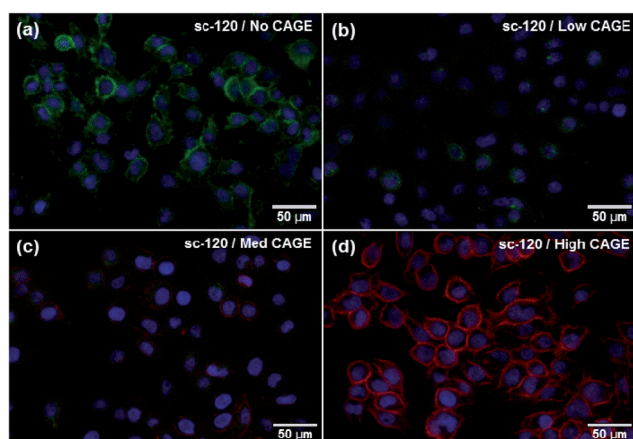

Fig. 8 Competition assay of CAGE probes (red) with the sc-120 AF488 EGFR antibody (green) for evaluation of specific binding affinity in 15B cells. (a) 1 : 50 sc-120 alone (b) 1 : 50 sc-120, 0.1 mg mL^{-1} of CAGE, (c) 1 : 50 sc-120, 0.8 mg mL^{-1} of CAGE, (d) 1 : 50 sc-120, 2 mg mL^{-1} of CAGE.

(commercial anti-EGFR antibody) in the presence of the linker protein avidin. The resulting CAGE probes are stable in solution and show minimal toxicity to cells. Using fluorescence-based *in vitro* assays, we have confirmed that the probes bind preferentially to EGFR+ cells compared to EGFR− cells. The MR relaxivity of these probes is sufficient to provide reasonable levels of positive contrast in MR images. In future studies, we will examine the binding of CAGE probes *in vivo* using animal models of SCCHN. The eventual goal is to use these probes to track the uptake of targeted agents in patients during the course of a typical 7-week cancer treatment. It is hoped that the tracking ability using MRI will eventually enable physicians to personalize the treatment for each patient and thereby help to improve outcomes for these patients.

Conflict of interest

The authors declare no competing financial interest.

Acknowledgements

References

1 R. C. Bast, Jr, C. M. Boyer, I. Jacobs, F. J. Xu, S. Wu, J. Wiener, M. Kohler and A. Berchuck, *Cancer*, 1993, **71**, 1597–1601.
2 J. Ishikawa, S. Maeda, K. Umezu, T. Sugiyama and S. Kamidono, *Int. J. Cancer*, 1990, **45**, 1018–1021.
3 J. W. Kim, Y. T. Kim, D. K. Kim, C. H. Song and J. W. Lee, *Gynecol. Oncol.*, 1996, **60**, 283–287.
4 K. Rikimaru, K. Tadokoro, T. Yamamoto, S. Enomoto and N. Tsuchida, *Head Neck*, 1992, **14**, 8–13.
5 K. W. Robertson, J. R. Reeves, G. Smith, W. N. Keith, B. W. Ozanne, T. G. Cooke and P. D. Stanton, *Cancer Res.*, 1996, **56**, 3823–3830.
6 B. Mukherjee, B. McEllin, C. V. Camacho, N. Tomimatsu, S. Sirasanagandala, S. Nannepaga, K. J. Hatanpaa, B. Mickey, C. Madden, E. Maher, D. A. Boothman, F. Furnari, W. K. Cavenee, R. M. Bachoo and S. Burma, *Cancer Res.*, 2009, **69**, 4252–4259.
7 M. Baumann and M. Krause, *Radiother. Oncol.*, 2004, **72**, 257–266.
8 Z. Liang, J. Zhang, X. Zeng, J. Gao, S. Wu and T. Liu, *BMC Cancer*, 2010, **10**, 376.
9 W. J. Pattje, E. Schuuring, M. F. Mastik, L. Slagter-Menkema, M. L. Schrijvers, S. Alessi, B. F. van der Laan, J. L. Roodenburg, J. A. Langendijk and J. E. van der Wal, *Br. J. Cancer*, 2010, **102**, 1778–1785.
10 J. A. Bonner, P. M. Harari, J. Giralt, R. B. Cohen, C. U. Jones, R. K. Sur, D. Raben, J. Baselga, S. A. Spencer, J. Zhu, H. Youssoufian, E. K. Rowinsky and K. K. Ang, *Lancet Oncol.*, 2010, **11**, 21–28.
11 T. Volkel, P. Holig, T. Merdan, R. Muller and R. E. Kontermann, *Biochim. Biophys. Acta*, 2004, **1663**, 158–166.
12 P. M. Harari and S. M. Huang, *Invest. New Drugs*, 1999, **17**, 259–269.
13 D. J. Jonker, C. J. O'Callaghan, C. S. Karapetis, J. R. Zalcberg, D. Tu, H. J. Au, S. R. Berry, M. Krahn, T. Price, R. J. Simes, N. C. Tebbutt, G. van Hazel, R. Wierzbicki, C. Langer and M. J. Moore, *N. Engl. J. Med.*, 2007, **357**, 2040–2048.
14 J. B. Vermorken, R. Mesia, F. Rivera, E. Remenar, A. Kawecki, S. Rottey, J. Erfan, D. Zabolotnyy, H. R. Kienzer, D. Cupissol, F. Peyrade, M. Benasso, I. Vynnychenko, D. De Raucourt, C. Bokemeyer, A. Schueler, N. Amellal and R. Hitt, *N. Engl. J. Med.*, 2008, **359**, 1116–1127.
15 R. Weissleder and M. J. Pittet, *Nature*, 2008, **452**, 580–589.
16 V. Darras, M. Nelea, F. M. Winnik and M. D. Buschmann, *Carbohydr. Polym.*, 2010, **80**, 1137–1146.
17 T. Fujimoto, H. Ichikawa, T. Akisue, I. Fujita, K. Kishimoto, H. Hara, M. Imabori, H. Kawamitsu, P. Sharma, S. C. Brown, B. M. Moudgil, M. Fujii, T. Yamamoto, M. Kurosaka and Y. Fukumori, *Applied radiation and isotopes: including data, instrumentation and methods for use in agriculture, industry and medicine*, 2009, vol. 67, pp. S355–358.
18 T. Nam, S. Park, S. Y. Lee, K. Park, K. Choi, I. C. Song, M. H. Han, J. J. Leary, S. A. Yuk, I. C. Kwon, K. Kim and S. Y. Jeong, *Bioconjugate Chem.*, 2010, **21**, 578–582.
19 I. Pashkunova-Martic, C. Kremser, M. Galanski, V. Arion, P. Debbage, W. Jaschke and B. Keppler, *Mol. Imag. Biol.*, 2011, **13**, 16–24.
20 T. Grobner and F. C. Prischl, *Kidney Int.*, 2007, **72**, 260–264.
21 H. J. Weinmann, R. C. Brasch, W. R. Press and G. E. Wesbey, *AJR, Am. J. Roentgenol.*, 1984, **142**, 619–624.
22 S. E. Cowper, P. H. Kuo and R. Bucala, *Arthritis Rheum.*, 2007, **56**, 3173–3175.
23 S. Petersen, O. Mohrs, G. Horstick, K. Oberholzer, N. Abegunewardene, K. Ruetzel, J. Selvanayagam, M. Robson, S. Neubauer, M. Thelen, J. Meyer and K. F. Kreitner, *J. Cardiovasc. Magn. Reson.*, 2004, **6**, 541–548.
24 A. D. Sherry, L. M. De Leon-Rodriguez, A. J. M. Lubag, C. R. Malloy, G. V. Martinez and R. J. Gillies, *Acc. Chem. Res.*, 2009, **42**, 948–957.
25 K. Luo, G. Liu, W. She, Q. Wang, G. Wang, B. He, H. Ai, Q. Gong, B. Song and Z. Gu, *Biomaterials*, 2011, **32**, 7951–7960.
26 K. Luo, G. Liu, B. He, Y. Wu, Q. Gong, B. Song, H. Ai and Z. Gu, *Biomaterials*, 2011, **32**, 2575–2585.
27 K. Luo, G. Liu, X. Zhang, W. She, B. He, Y. Nie, L. Li, Y. Wu, Z. Zhang, Q. Gong, F. Gao, B. Song, H. Ai and Z. Gu, *Macromol. Biosci.*, 2009, **9**, 1227–1236.
28 M. F. Bellin, *Eur. J. Radiol.*, 2006, **60**, 314–323.
29 H. T. Chen, M. F. Neerman, A. R. Parrish and E. E. Simanek, *J. Am. Chem. Soc.*, 2004, **126**, 10044–10048.
30 K. B. Ghaghada, M. Ravoori, D. Sabapathy, J. Bankson, V. Kundra and A. Annapragada, *PLoS One*, 2009, **4**, e7628.
31 M. C. Woodle, L. R. Collins, E. Sponsler, N. Kossovsky, D. Papahadjopoulos and F. J. Martin, *Biophys. J.*, 1992, **61**, 902–910.

32 P. Caravan, *Chem. Soc. Rev.*, 2006, **35**, 512–523.

33 M. Ye, Y. Qian, J. Tang, H. Hu, M. Sui and Y. Shen, *J. Controlled Release*, 2013, **169**, 239–245.

34 Z. Cheng, D. L. Thorek and A. Tsourkas, *Angew. Chem., Int. Ed.*, 2010, **49**, 346–350.

35 J. R. Grandis and D. J. Tweardy, *Cancer Res.*, 1993, **53**, 3579–3584.

36 S. Kalyankrishna and J. R. Grandis, *J. Clin. Oncol.*, 2006, **24**, 2666–2672.

37 J. E. M. van Leeuwen and H. A. J. Alwan, *J. Biol. Chem.*, 2007, **282**, 1658–1669.

38 W. J. Luo, Y. M. Zhang, X. Li and X. M. Xu, *Afr. J. Biotechnol.*, 2010, **9**, 4674–4680.

39 M. C. Filion and N. C. Phillips, *Biochim. Biophys. Acta*, 1997, **1329**, 345–356.

40 G. Smistad, J. Jacobsen and S. A. Sande, *Int. J. Pharm.*, 2007, **330**, 14–22.

41 W. J. Mulder, G. J. Strijkers, A. W. Griffioen, L. van Bloois, G. Molema, G. Storm, G. A. Koning and K. Nicolay, *Bioconjugate Chem.*, 2004, **15**, 799–806.